



Original

Microwave sintering of tungsten heavy alloys

G. Prabhu*, M. Sankaranarayana, T. K. Nandy

Defence Metallurgical Research Laboratory, P.O.Kanchanbagh, Hyderabad-500059, India.

Received dd mm aaaa; accepted dd mm aaaa
Available online dd mm aaaa

Abstract: To understand microwave sintering of heavy alloys with high tungsten content, 93W-4.9Ni-2.1Fe alloy was sintered using a 6 kW, 2.45 GHz microwave sintering furnace at 1783 K (1510 °C) and 1793 K (1520 °C). The alloy sintered at 1793 K (1520 °C) achieved full densification and had improved microstructural features, superior mechanical properties compared to 99.4% densification and relatively inferior properties obtained in the alloy sintered at 1783 K (1510 °C). This study also includes a comparison between microwave sintered and conventionally sintered 93W-4.9Ni-2.1Fe alloy (sintered at 1793K (1520°C)). Contrary to the full densification and superior mechanical properties obtained in microwave sintering, conventional sintering at 1793K (1520°C) resulted in only 99.6% densification and substantially inferior properties. Analyses of microstructure and fracture surface revealed that key microstructural parameters such as tungsten grain size, tungsten-tungsten contiguity, matrix volume fraction and also the fracture mode were significantly different between the alloys processed by the two routes. Possible reasons behind dissimilar densification, significantly different microstructures and mechanical properties obtained between these two modes of sintering, are also discussed in this study.

Keywords: tungsten content, microwave sintering, contiguity

1. INTRODUCTION

Tungsten content plays a crucial role in choosing a heavy alloy composition since the sintering parameters, microstructural features and the final mechanical properties of a heavy alloy are largely influenced by the tungsten content. Gero, Borukhin, & Pikus (2001) have studied the correlation between the tungsten content and mechanical properties of conventionally sintered tungsten

heavy alloys with 90, 93 and 95 wt % tungsten and reported that the tungsten content has a major influence on the deformation and fracture behaviour of these alloys and the material plasticity increases substantially with decreasing tungsten content. Kiran et al. (2013) have reported similar observations in cobalt containing tungsten heavy alloys.

In terms of the processing method, conventional liquid phase sintering of heavy alloys usually involves prolonged holding time at the respective sintering temperature in order to achieve full densification. (Bose & German 1988) have reported that tungsten heavy alloys, thus sintered by conventional methods, have coarse tungsten grains with

* Corresponding author.

E-mail address: prabhu83@gmail.com (G. Prabhu).

grain size in the range of 20 to 60 μm . Kim, Lee, Ryu, Hyunghong, and Noh (2000) have mentioned that coarse tungsten grain can be attributed to the deterioration of mechanical properties in heavy alloys. Hence, the window for processing tungsten heavy alloys, especially high tungsten content alloys using optimum sintering temperature and time, is usually narrow. In order to alleviate the adverse effects of long sintering time, microwave sintering and spark plasma sintering which use faster heating rates resulting in finer microstructures, are being considered as possible alternate methods to process tungsten heavy alloys.

Upadhyaya, Tiwari, and Mishra (2007) and Li, Hu, Li, Ai, Qu (2013) have reported microwave sintering and spark plasma sintering of tungsten heavy alloys respectively. Authors, in their earlier work (Prabhu, Kumar, Sankaranarayana, & Nandy, 2014), have also reported microwave sintering of 90W-7Ni-3Fe and 90W-6Ni-2Fe-2Co alloys at 1733 K (1460 °C) and 1743 K (1470 °C) respectively. Liu, Ma, & Zhang (2012) and Ma, Zhang, Liu, Yue, and Huang (2014) have also studied 93W-4.9Ni-2.1Fe alloy under microwave sintering between 1523 K (1250°C) and 1823 K (1550°C).

In addition to tungsten content, sintering parameters in the case of microwave sintering, are significantly influenced by the volume of the samples since the heating mechanism in microwave sintering is ‘volumetric heating’ (Li, Hu, Qu, Li, & Yang, 2014). Any substantial change in the dimensions and thereby the volume of the samples necessitates corresponding change in sintering parameters in order to achieve complete densification. Liu et al. (2012) have studied microwave sintering of 93W-4.9Ni-2.1Fe alloy between 1523 K (1250°C) and 1773 K (1500°C) for 5 minutes, using a 4.5g tensile sample. The importance of sintering parameters is clearly evident even in such smaller volumes; the samples exhibit porosity (90 % densification) and inferior properties at 1523 K (1250°C) compared to 98.8% densification and superior properties at 1773 K (1500°C). Ma et al. (2014) have also reported microwave sintering of 93W-4.9Ni-2.1Fe alloy at 1823 K (1550°C) for 30 minutes, using samples in the form of extruded rods with 24 mm diameter. It is observed from these investigations that within a single alloy composition of 93W-4.9Ni-2.1Fe, the sintering parameters are dependent on the volume of the samples. Thus, microwave sintering of high tungsten content heavy alloys becomes a challenging task, with both tungsten content and sample

volume playing vital role in influencing the sintering parameters.

In the present study, samples of dimensions 40 mm diameter and 70 mm height (in green stage) are microwave sintered at 1783 K (1510 °C) and 1793 K (1520 °C) in an effort to determine the optimum sintering parameters for this particular sized 93W-4.9Ni-2.1Fe alloy. The present study also attempts at understanding the two different modes of sintering, namely, conventional and microwave, in the case of 93W-4.9Ni-2.1Fe alloy, using a sintering temperature of 1793 K (1520 °C).

2. EXPERIMENTAL

Commercially available elemental powders of tungsten, nickel and iron with 99.95 pct purity and average particle size $D_{50}=17.3$, 9.5 and 11.6 μm respectively, were used to obtain 93W-4.9Ni-2.1Fe alloy. Details of the powders used in the present study are tabulated in Table 1.

Table 1.
Properties of tungsten, nickel and iron powders (as-received grade).

Properties	Tungsten	Nickel	Iron
Apparent density, g cm^{-3}	4.7	2.1	3
Tap density, g cm^{-3}	7.1	4.2	4.2
Particle Shape	Cuboidal	Irregular	Spherical
Particle size (D_{50}), μm	17.3	9.5	11.6

Particle morphology of the powders was studied using scanning electron microscopy (Make: FEI Quanta 400 ESEM) and is shown in Figure 1 (a-c).

The powders were mixed for 24 hours in a conventional ball mill using stainless steel balls with 1:1 Ball to Powder Ratio (BPR). Subsequently, the powder mix was reduced in hydrogen atmosphere at 973 K (700°C) for 2 hours followed by cold isostatic pressing (Make: National Forge, Belgium, Capacity: 520 MPa) at 200 MPa without any binder. Size of the green compacts was maintained at 40 mm diameter and 70 mm length.

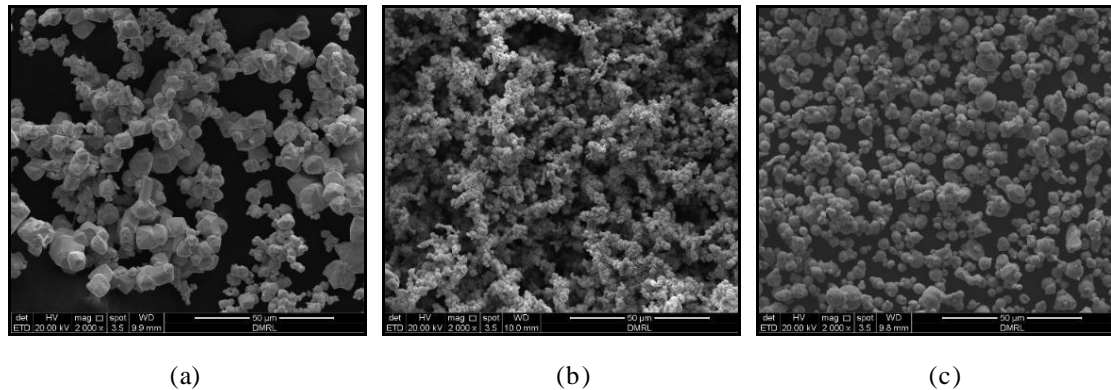


Fig. 1. Scanning electron microscopy images of as-received (a) tungsten powder (b) nickel powder and (c) iron powder.

Microwave sintering was carried out at 1783 K (1510°C) and 1793 K (1520°C) in a 6 kW, 2.45 GHz multimode microwave furnace (Make: Enerzi Microwave systems, India) with holding time of 60 minutes at the sintering temperature. Alumina casket was used as the sample holder and SiC as the susceptor. Heating rate was maintained at 20 K min⁻¹ (20°C min⁻¹) and sintering was carried out in hydrogen atmosphere.

Conventional sintering was carried out in a pusher type furnace (Make: FHD Furnaces Ltd, England) in hydrogen atmosphere at 1793 K (1520°C) with holding time of 60 minutes at the sintering temperature. The heating rate was maintained between 3 and 5 K min⁻¹ (3 and 5°C min⁻¹).

Density of the sintered samples was measured in a Mettler Balance, using Archimedes Principle (Make: Mettler, Capacity 2.4 kg). Sintered samples were mounted, polished and microstructural study was carried out using scanning electron microscope. Grain size, matrix volume fraction and dihedral angle measurements were made using Image analysis (Make: Image J). Contiguity was calculated using the formula $[2N_{WW} / (2N_{WW} + N_{WM})]$ wherein (N_{WW}) is the number of tungsten-tungsten contacts and (N_{WM}) the number of tungsten-matrix contacts. N_{WW} and N_{WM} were determined using the line intercept method wherein grid lines were placed on the microstructure image and the number of contact points was counted. 100 measurements were made using the line intercept method to determine contiguity. Tensile samples prepared as per ASTM standard E8-T11 (2003) were tested in a tensometer (Make: Monsanto, Capacity: 2000 kg). Charpy impact testing was carried out using unnotched specimens of dimensions 10 mm x 10 mm x 55 mm in impact testing machine (Make: Fuel Instruments-India, Model: IT 30 ASTM, 0-300 J). Fracture surfaces of

the failed tensile tested and impact tested samples were also studied using scanning electron microscopy.

3. RESULTS

Microstructures of 93W-4.9Ni-2.1Fe alloy, microwave sintered at 1783 K (1510°C), 1793 K (1520°C) and conventionally sintered at 1793 K (1520°C) are shown in Figure 2 (a-c).

Microwave sintering of 93W-4.9Ni-2.1Fe alloy at 1783 K (1510°C) has resulted in a relative density of 99.4% and porosity is observed between the tungsten grains (shown in Figure 2(a)) whereas at 1793 K (1520°C) pores are completely eliminated (shown in Fig.2(b)) and the alloy achieved full densification. Though similar average grain size is observed in both the alloys, the shape of tungsten grains is polygonal at 1783 K (1510°C) and near-spherical at 1793 K (1520°C). In addition, the alloy sintered at 1783 K (1510°C) has higher contiguity, higher dihedral angle and lesser matrix volume fraction (listed in Table 2) compared to the alloy sintered at 1793 K (1520°C).

Conventional sintering carried out at 1793 K (1520°C) has resulted in only 99.6% densification and unlike the microwave sintered alloy, the microstructure of the conventionally sintered alloy (shown in Figure 2(c)) shows presence of porosity and coarse, polygonal tungsten grains of substantially higher average grain size (listed in Table 2). Other key microstructural parameters like contiguity, dihedral angle are also higher and the matrix volume fraction (listed in Table 2) is significantly lower compared to the microwave sintered alloy. Mechanical properties of microwave sintered and conventionally sintered 93W-4.9Ni-2.1Fe alloy are listed in Table 2.

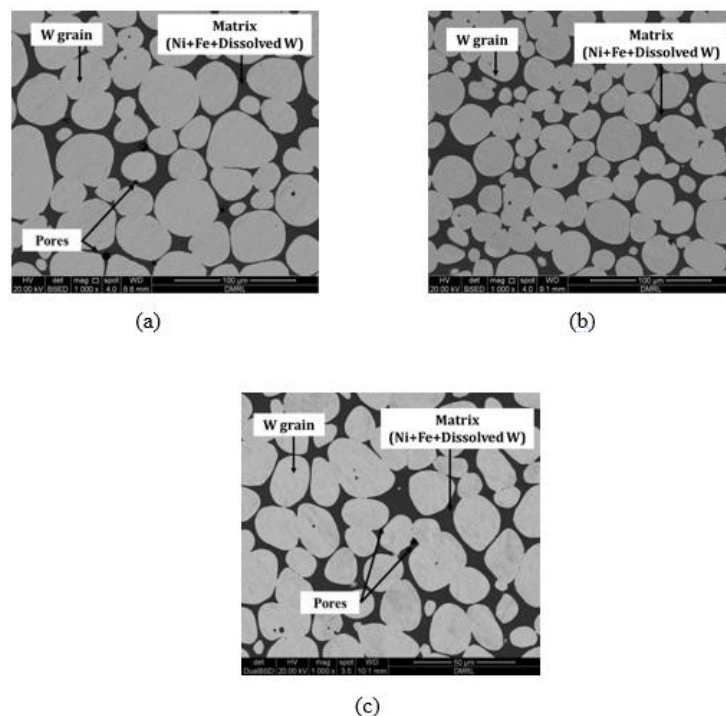


Fig. 2. Microstructures of 93W-4.9Ni-2.1Fe alloy (a) microwave sintered at 1783 K (1510°C), (b) microwave sintered at 1793 K (1520°C) and (c) conventionally sintered at 1793 K (1520°C).

Table 2.

Comparison of microstructural features and mechanical properties between microwave sintered and conventionally sintered 93W-4.9Ni-2.1Fe alloys.

Microstructural features and mechanical properties	Microwave sintered at 1783 K (1510°C)	Microwave sintered at 1793 K (1520°C)	Conventionally sintered at 1793 K (1520°C)
Average grain size (μm)	29 ± 13	29 ± 12	37 ± 16
Contiguity	0.29	0.2	0.34
Dihedral angle (deg.)	48 ± 25	26 ± 9	43 ± 19
Matrix volume fraction (vol %)	12.5	20.7	9.7
UTS, MPa	736	843	683
%elongation	5	13	3
Impact toughness, J/cm ²	140	176	14

In terms of the tensile properties, between the microwave sintered alloys, the alloy sintered at 1783 K (1510°C) has lower ultimate tensile strength and elongation (listed in Table 2) compared to the alloy sintered at 1793 K (1520°C). Fractographs of failed tensile

sintered at 1793 K (1520°C). Fractographs of failed tensile specimens of both the microwave sintered and conventionally alloys are shown in Figure 3 (a-c).

Fracture surface of the alloy microwave sintered at 1783 K (1510°C) exhibits both intergranular and

transgranular failure (shown in Figure 3 (a)). Features of intergranular failure such as (i) tungsten-tungsten debonding, (ii) tungsten-matrix decohesion and (iii) instances of isolated matrix rupture are observed in the fractograph (shown in Figure 3(a)). Tungsten-matrix decohesion leaves the tungsten grains intact, which is also clearly evident in the tensile fractograph shown in Figure 3 (a). In addition, cleavage of tungsten grains and secondary crack propagation through the tungsten grain are also observed (shown in Figure 3 (a)) which indicate that transgranular failure has also occurred in the alloy. Contrarily, in the alloy microwave sintered at a marginally higher temperature of 1793 K (1520°C), the fracture mode is predominantly transgranular with fewer instances of intergranular failure, as shown in Figure 3 (b). In the tensile fractograph shown in Figure 3(b), features of transgranular failure such as (i) tungsten grain cleavage (ii) secondary crack propagation indicating failure of tungsten grains are the dominant features observed compared to the intergranular-failure features such as tungsten-tungsten debonding and tungsten-matrix decohesion.

Conventionally sintered alloy, though sintered at 1793 K (1520°C), has the least tensile strength and elongation (listed in Table 2) among all the three alloys. The tensile fractograph (shown in Figure 3(c)) shows features of

predominant intergranular failure with very rare occurrences of transgranular failure. Tungsten-tungsten debonding, tungsten-matrix decohesion and isolated matrix rupture are certainly more prevalent than tungsten grain cleavage.

Charpy impact toughness values of all the three alloys are listed in Table 2. Fractographs of failed impact specimens of both the microwave sintered and conventionally alloy are shown in Figure 4 (a-c). Impact fractographs of both the microwave sintered alloys (shown in Figure 4(a) and 4(b)) have similar features, namely, (i) river-line patterns in tungsten grains indicating transgranular failure (ii) ductile failure of the matrix characterized by dimples or tearing and (iii) tungsten-tungsten debonding indicating intergranular failure.

The alloy sintered at 1783 K (1510°C) has more frequent occurrences of tungsten-tungsten debonding whereas the alloy sintered at 1793 K (1520°C) has more instances of grain cleavage and ductile-dimple failure of the matrix. Conventionally sintered alloy has the least impact toughness (listed in Table 2) among the three alloys studied. Unlike the microwave sintered alloys which show both transgranular and intergranular failure, the conventionally sintered alloy shows ample evidence of intergranular failure indicated by tungsten-tungsten debonding (shown in Figure 4(c)).

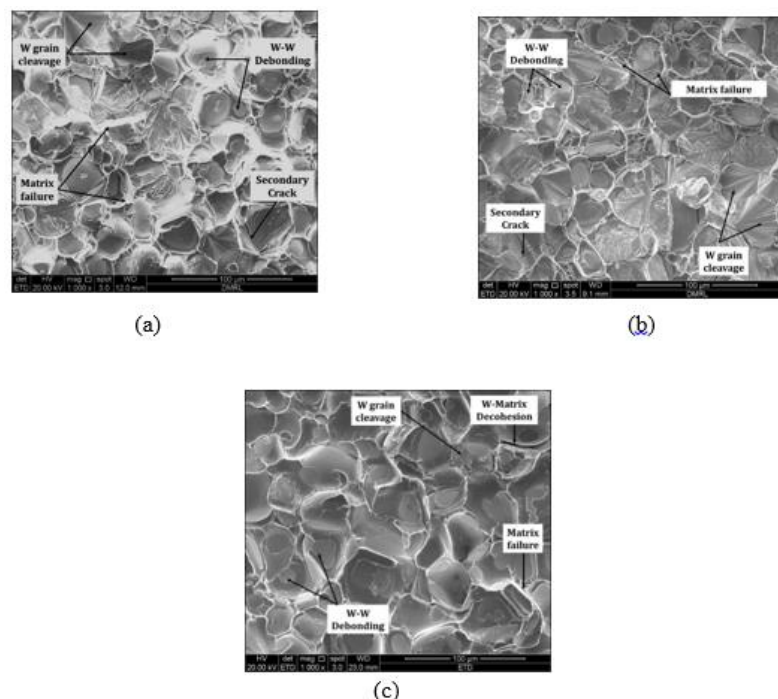


Fig. 3. Tensile fractographs of 93W-4.9Ni-2.1Fe alloy (a) microwave sintered at 1783 K (1510°C), (b) microwave sintered at 1793 K (1520°C) and (c) conventionally sintered at 1793 K (1520°C).

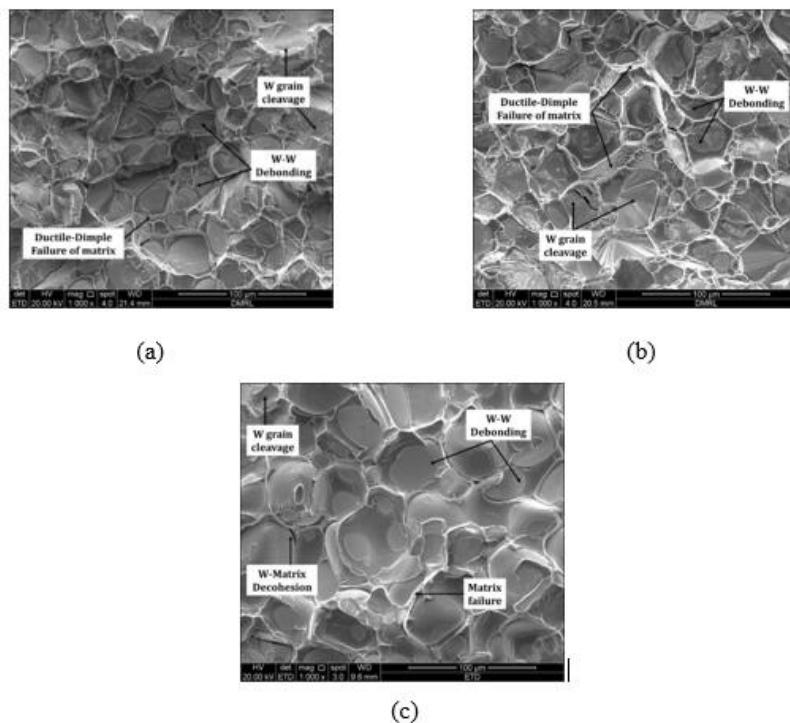


Fig. 4. Impact fractographs of 93W-4.9Ni-2.1Fe alloy (a) microwave sintered at 1783 K (1510°C), (b) microwave sintered at 1793 K (1520°C) and (c) conventionally sintered at 1793 K (1520°C).

4. DISCUSSION

4.1 MICROSTRUCTURE

In the alloy microwave sintered at 1783 K (1510°C), pores observed between the tungsten grains (shown in Figure 2(a)) indicate that the matrix has not completely penetrated between the tungsten grains. Lower sintering temperature of 1783 K (1510°C) could possibly be the reason behind incomplete matrix penetration and consequently the presence of porosity. On the contrary, at higher temperature of 1793 K (1520°C), pores are completely eliminated, tungsten grains and matrix are more evenly distributed and matrix has penetrated between most of the tungsten grains (shown in Figure 2(b)). With marginal increase in the temperature, matrix (liquid) fluidity is expected to improve and the rearrangement of tungsten grains, dissolution-reprecipitation are enhanced resulting in uniform distribution of grains and matrix. Liu, Ma, & Cai (2011) have made similar observations in 93W-4.9Ni-2.1Fe alloy microwave sintered at 1773 K (1500°C). It is reported that at 1773 K (1500°C), liquid flow and particle

rearrangement are insufficient resulting in non-uniform distribution of angular shaped tungsten grains in the matrix. However, if the sintering temperature is increased up to 1823 K (1550°C), matrix (liquid phase) flow, migration and rearrangement of tungsten grains, dissolution and reprecipitation are quite significant resulting in complete densification and near-spherical tungsten grains. Very similar to the observations made by Liu et al. (2011) in terms of grain shape, it is also observed in the present study that though average grain size is similar in both the alloys, most of the tungsten grains are angular shaped at 1783 K (1510°C) compared to the presence of a number of near-spherical grains at 1793 K (1520°C).

Park, Baik, Kang, and Yoon (1996) have reported that if the volume fraction of the matrix is sufficiently high, the grains would be nearly spherical in shape, but with low matrix volume fraction the grains accommodate their shape to their neighbours and become angular. Similar observations are made in the present study; the alloy microwave sintered at 1783 K (1510°C) has substantially lower matrix volume fraction (listed in Table 2) and the rearrangement of tungsten grains within this low matrix

volume fraction has resulted in angular shaped tungsten grains (shown in Figure 2(a)) whereas at 1793 K (1520°C), the matrix volume fraction is sufficiently high for the tungsten grains to distribute more evenly and transform to near-spherical shape by Ostwald ripening mechanism.

In terms of other key microstructural parameters such as dihedral angle and contiguity, the alloy microwave sintered at 1783 K (1510°C) has higher dihedral angle and contiguity (listed in Table 2) compared to the alloy microwave sintered at 1793 K (1520°C). Rabin & German (1988) have reported that dihedral angle; the ratio between the solid-solid and solid-liquid interfacial energies, is dependent on sintering temperature. With increasing temperature, the solid-liquid interfacial energy decreases more rapidly than the solid-solid interfacial energy and hence dihedral angle decreases with increase in sintering temperature (Rabin & German, 1988). Liu & German (2001) reported that a low dihedral angle system has low solid-liquid interfacial energy and hence favours liquid penetration between the solid-solid contacts. In the present study, among the microwave sintered alloys, the dihedral angle (listed in Table 2) is found to decrease with increase in temperature from 1783 K (1510 °C) to 1793 K (1520 °C). Low dihedral angle obtained at 1793 K (1520°C) has favoured matrix (liquid) penetration between the tungsten grains and the grains are separated by the matrix resulting in low contiguity.

Contiguity, as reported by German (1985), is the quantitative measurement of interphase contact. In the case of tungsten heavy alloys, the number of contact points between tungsten-tungsten grains are measured and defined as contiguity. German (1985) has also reported that contiguity has strong dependence on dihedral angle and it increases with increase in dihedral angle. In the present study, a similar trend is observed; the alloy microwave sintered at 1783 K (1510°C) has high dihedral angle between the grains and hence has higher contiguity whereas the alloy microwave sintered at 1793 K (1520°C) has lower dihedral angle and hence lower contiguity.

4.2 MECHANICAL PROPERTIES

Tungsten-Tungsten contiguity is a major factor influencing both tensile and impact properties of heavy alloys. Humail, Akhtar, Askari, Tufail, & Qu (2007) have reported that these properties show a decreasing trend

with increasing contiguity. Churn & German (1984) have reported the relationship between elongation to failure and contiguity as $\epsilon_f = K_2(1 - C_w)$ where ϵ_f is the elongation to failure, K_2 is a material constant and C_w is the contiguity. In the present study, between the microwave sintered alloys, elongation and contiguity follow a similar trend; the alloy sintered at 1783 K (1510°C) exhibits higher contiguity and consequently lower elongation (listed in Table 2) whereas the alloy sintered at 1793 K (1520°C) has higher elongation owing to its lower contiguity. In terms of the ultimate tensile strength (listed in Table 2), in the alloy sintered at 1783 K (1510°C), presence of contiguous tungsten grains and porosity result in premature failure in tensile loading and hence lower tensile strength is observed. Thus, a combination of superior tensile strength and elongation is achieved in the alloy sintered at 1793 K (1520°C) compared to the alloy sintered at 1783 K (1510°C). Authors, in their earlier work (Prabhu et al., 2014) have also reported similar observations on the effect of contiguity on the tensile properties of 90W-7Ni-3Fe and 90W-6Ni-2Fe-2Co alloys. A comparative plot of the tensile properties obtained in the present study and in the authors' previous work (Prabhu et al., 2014) is shown in Figure 5.

In terms of tensile fractography, fracture modes of tungsten heavy alloys can be classified as: (i) debonding along tungsten-tungsten interface, (ii) decohesion along tungsten-matrix interface, (iii) tungsten grain cleavage and (iv) matrix failure (Churn & German, 1984). Tungsten-tungsten interface, being the weakest interface is the crack initiation site whereas crack propagation can occur in one of the following two modes; (i) intergranular failure, if weak tungsten-tungsten interfaces are abundant and the tungsten-matrix interface is also not strong enough to stop crack propagation, then the crack propagates along these interfaces, leaving the tungsten grains intact and (ii) transgranular failure, if weak tungsten-tungsten interfaces are less frequent and tungsten-matrix interface is strong enough to stop interfacial crack propagation, then the crack moves within the grain resulting in grain cleavage (Churn & German 1984). In terms of the properties obtained in these two modes of failure, intergranular failure results in inferior properties compared to transgranular failure.

Authors, in their earlier work (Prabhu et al., 2014) have reported transgranular failure and superior tensile

properties in the case of microwave sintered 90W7Ni-3Fe and 90W-6Ni-2Fe-2Co alloys compared to intergranular failure and inferior tensile properties in conventionally sintered alloys.

In the present study, between the microwave sintered alloys, the alloy sintered at 1783 K (1510°C) does not exhibit a single dominant failure mode, instead, the fractograph has features of both intergranular and transgranular failure (shown in Figure 3(a)). Features of intergranular failure such as tungsten-tungsten debonding, tungsten-matrix decohesion and isolated matrix rupture are observed along with tungsten grain cleavage and secondary crack propagation which indicate transgranular failure (shown in Figure 3(a)). Contrarily, in the case of the alloy sintered at 1793 K (1520°C), tungsten grain cleavage and crack propagation through the grain are dominant compared to limited occurrences of tungsten-tungsten debonding (shown in Figure 3(b)). The tensile properties (listed in Table 2) obtained are in agreement with the tensile fractographs; the alloy sintered at 1793 K (1520°C) has predominant transgranular failure and superior properties compared to the alloy sintered at 1783 K (1510°C) which has both intergranular, transgranular failure and hence relatively inferior properties.

Contiguity, apart from affecting the tensile properties, has also been reported to be a major factor influencing the impact toughness of a tungsten heavy alloy (Das, Kiran, Chakraborty, & Prasad, 2009). Joonwoong et al. (1993) have reported that with increasing matrix penetration (or decreasing tungsten-tungsten interfacial area or low contiguity) the fraction of ductile-dimple failure of the matrix increases, implying that the plastic deformation of the additional matrix phase along the crack propagation

increases the impact energy. Under high strain rate loading such as impact loading, the matrix phase undergoes ductile - dimple fracture whereas tungsten grains fail by cleavage (Joonwoong et al., 1993). Impact toughness values of the microwave sintered alloys are listed in Table 2. The alloy sintered at 1783 K (1510°C) has higher contiguity, lower matrix volume fraction (listed in Table 2) and hence lower impact toughness compared to the alloy sintered at 1793 K (1520°C).

Impact fractographs of both the alloys are shown in Figure 4(a) and 4(b). Though both the alloys exhibit the following features; (i) tungsten grain cleavage, (ii) ductile-dimple failure of the matrix and (iii) tungsten-tungsten debonding, the alloy sintered at 1783 K (1510°C) has more frequent instances of tungsten-tungsten debonding compared to the alloy sintered at 1793 K (1520°C). This observation indicates that the dominant mode of failure is intergranular in the alloy sintered at 1783 K (1510°C), thereby explaining the marginally lower impact toughness (listed in Table 2) obtained in the alloy.

In case of the alloy sintered at 1793 K (1520°C), tungsten grain cleavage and ductile-dimple failure of the matrix are the major features observed compared to tungsten-tungsten debonding. Increase in the impact toughness of the alloy sintered at 1793 K (1520°C) can be attributed to lower contiguity and higher matrix volume fraction. Authors, in their earlier work (Prabhu et al., 2014) have also reported similar observations on the effect of contiguity on the impact toughness of 90W-7Ni-3Fe and 90W-6Ni-2Fe-2Co alloys. A comparative plot of impact toughness of microwave sintered alloys obtained in the present study and in the authors' previous work (Prabhu et al., 2014) is shown in Figure 6.

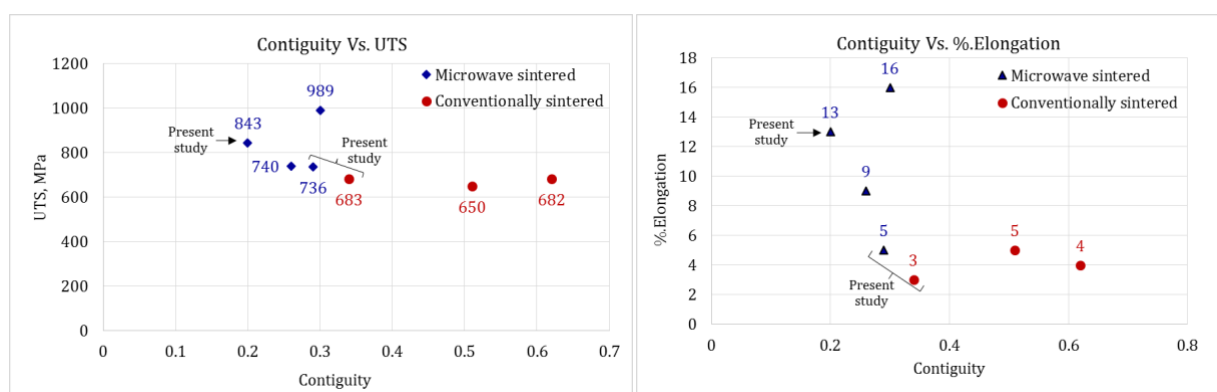


Fig. 5. Effect of contiguity on tensile properties of heavy alloys. Present study and literature (Prabhu et al., 2014) values are plotted.

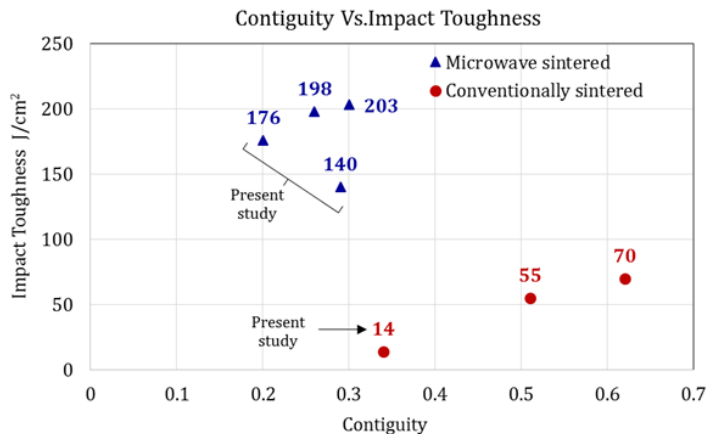


Fig. 6. Effect of contiguity on impact toughness of heavy alloys. Present study and literature (Prabhu et al., 2014) values are plotted.

4.3 COMPARISON WITH CONVENTIONAL SINTERING

In order to compare microwave and conventional sintering, particularly in the case of high tungsten content heavy alloys, 93W-4.9Ni-2.1Fe alloy is sintered in conventional sintering mode using the same sintering parameters of 1793 K (1520°C) and holding time of 60 min. The heating rate used in microwave sintering process is 20 K min^{-1} ($20^\circ\text{C min}^{-1}$) and in the conventional sintering process is 3 to 5 K min^{-1} (3 to 5°C min^{-1}). Authors in their earlier work have studied the effect of similar heating rate by using 20 K min^{-1} ($20^\circ\text{C min}^{-1}$) in these two modes of sintering using 90W-7Ni-3Fe, 90W-6Ni-2Fe-2Co alloys and have reported that higher heating rate of 20 K min^{-1} ($20^\circ\text{C min}^{-1}$) in conventional sintering results in highly contiguous, irregular tungsten grains and inferior properties (Prabhu et al., 2014). Hence heating rate of 3 to 5 K min^{-1} (3 to 5°C min^{-1}) is being used in the present study in the case of conventional sintering.

Contrary to the full densification and desirable microstructure obtained at 1793 K (1520°C) in the case of microwave sintering, conventional sintering has resulted in only 99.6% densification and partially developed microstructural features. Porosity is observed between the tungsten grains (shown in Figure 2(c)). Though the sintering parameters of 1793 K (1520°C)/60 min are the same for both the alloys, the conventionally sintered alloy has coarse tungsten grains, higher dihedral angle, higher contiguity and lower matrix volume fraction (listed in Table 2) compared to the microwave sintered alloy.

Possible reasons for the dissimilar microstructural features obtained between the two modes of sintering could be the heating mechanism and the sintering time. Unlike microwave sintering which involves volumetric heating, conventional sintering involves heat transfer from the surface to the core of the sample. With the absence of volumetric heating, sufficient time has to be provided in conventional sintering for heat transfer to occur over the entire sample and result in full densification and desirable microstructural changes. In the present study, though the heating rate is 3 to 5 K min^{-1} (3 to 5°C min^{-1}), the holding time of 60 min proves to be inadequate for complete densification and microstructure development. Hence, the alloy conventionally sintered at 1793 K (1520°C) does not have a fully developed microstructure (shown in Figure 2(c)) primarily because of the reduced processing time.

Another factor that contributes towards microstructure development is the dissolution of tungsten in the matrix. Liu et al. (2012) have reported that microwave energy accelerates dissolution of tungsten in the matrix. Though the mechanism is not clearly understood, it has also been observed by the authors in their previous work (Prabhu et al., 2014) that dissolution of tungsten in the matrix is higher in microwave sintered alloys compared to conventionally sintered alloys. Enhanced tungsten dissolution in the matrix (or higher solid solubility in the liquid) facilitates matrix penetration between the grains thereby decreasing the dihedral angle. Tungsten grains are thus separated by the liquid phase resulting in decrease of tungsten-tungsten contiguity.

Thus microwave sintered alloys have lower contiguity compared to conventionally sintered alloys.

Influence of contiguity on tensile properties, which has been discussed earlier, is also observed in the conventionally sintered alloy. Conventionally sintered alloy has substantially inferior tensile strength and elongation (listed in Table 2) owing to the presence of presence of porosity, contiguous tungsten grain network and low matrix volume fraction. Fracture surfaces of tensile tested samples of both microwave and conventionally sintered alloy are shown in Figure 3(a) and 3(c). Microwave sintered alloy, as mentioned earlier, has predominant transgranular failure and hence superior mechanical properties whereas conventionally sintered alloy exhibits predominant intergranular failure and as expected inferior tensile properties. Thus, the fractographic features (as shown in Figure 3(a) and 3(c)) of both the microwave sintered and conventionally sintered alloys are found to be consistent with their tensile properties.

In terms of impact toughness, microwave sintered alloy has substantially higher impact value (176 J/cm^2) compared to the conventionally sintered alloy (14 J/cm^2). Matrix penetration between the tungsten grains (indicated by contiguity and dihedral angle) can be attributed to the varying impact toughness values obtained between the microwave and conventional alloys. Microwave sintered alloy, with lower contiguity and dihedral angle has sufficient matrix penetration between the tungsten grains and hence higher impact toughness whereas higher contiguity and higher dihedral angle result in lower impact toughness in conventionally sintered alloy. Similar observations on impact toughness reported by the authors (Prabhu et al., 2014) is compared with the present study in Figure 6.

Impact fractographs are shown in Figure 4(a) and 4(c). The observations made in impact fractographs are very similar to those made using tensile fractographs. Microwave sintered alloy exhibits transgranular failure of the tungsten grains and ductile-dimple failure of the matrix (shown in Figure 4(a)). Conventionally sintered alloy does not show any evidence of grain cleavage and matrix failure; instead the alloy exhibits intergranular failure where the grains are separated along the weak tungsten-tungsten and tungsten-matrix interfaces leaving the tungsten grains intact (shown in Figure 4(c)).

Though the sintering temperature, holding time are exactly the same, the conventionally sintered alloy shows neither improved microstructure nor superior properties as compared to the microwave sintered alloy. Superior microstructure and mechanical properties in microwave sintered alloy are possibly because of the lesser sintering time involved owing to the volumetric heating mechanism.

Thus it is apparent that microwave sintered alloys will exhibit favourable microstructural features if sintering is carried out at appropriate temperatures. This in turn will have extremely favourable implications with regards to mechanical properties. Thus, there is a need to develop microwave furnaces in the lines of conventional sintering furnaces so that large number of microwave sintered alloys can be produced in a short time for the process to be economically viable.

5. CONCLUSIONS

Microwave sintering of 93W-4.9Ni-2.1Fe alloy at 1793 K (1520°C) resulted in full densification and improved microstructural features compared to the alloy sintered at 1783 K (1510°C). Superior tensile and impact properties obtained in the alloy sintered at 1793 K (1520°C) can be attributed to its microstructural features whereas the presence of porosity, high contiguity and low matrix volume fraction resulted in inferior tensile and impact properties in the alloy sintered at 1783 K (1510°C).

Contrary to the full densification and desirable microstructure obtained at 1793 K (1520°C) in the case of microwave sintering, conventional sintering at the same temperature has resulted in only 99.6% densification and partially developed microstructural features. This observation indicates that, in conventional sintering, tungsten heavy alloys need to be processed with sufficient sintering/holding time so as to facilitate microstructural changes like dissolution reprecipitation, rounding of tungsten grains. Tensile and impact properties of the conventionally sintered alloy are substantially inferior to the microwave sintered alloy because of the presence of porosity, contiguous tungsten grain network and low matrix volume fraction.

Based on the above observations, it is clearly evident that microwave sintering results in favourable microstructure and better mechanical properties in tungsten heavy alloys. Additionally, unlike conventional sintering, microwave sintering offers lesser processing time and energy consumption.

ACKNOWLEDGEMENTS

Authors would like to thank Defence Research and Development Organization for sponsoring the activity through a research project. Authors are thankful to the Director, DMRL for his encouragement and valuable guidance. We also thank all the technical staff of DMRL for their valuable contribution.

CONFLICT OF INTEREST

The authors have no conflicts of interest to declare.

REFERENCES

Bose, A., & German, R. M. (1988). Sintering atmosphere effects on tensile properties of heavy alloys. *Metallurgical Transactions A*, 19(10), 2467-2476.

Churn, K.S., German, R.M. (1984). Fracture behaviour of W-Ni-Fe heavy alloys. *Metallurgical transactions. A, Physical metallurgy and materials science*, 15 A (2), 331-338.

Das, J., Kiran, U. R., Chakraborty, A., & Prasad, N. E. (2009). Hardness and tensile properties of tungsten based heavy alloys prepared by liquid phase sintering technique. *International Journal of Refractory Metals and Hard Materials*, 27(3), 577-583.

Gero, R., Borukhin, L., & Pikus, I. (2001). Some structural effects of plastic deformation on tungsten heavy metal alloys. *Materials Science and Engineering: A*, 302(1), 162-167.

German, R. M. (1985). The contiguity of liquid phase sintered microstructures. *Metallurgical Transactions A*, 16(7), 1247-1252.

Humail, I. S., Akhtar, F., Askari, S. J., Tufail, M., & Qu, X. (2007). Tensile behavior change depending on the varying tungsten content of W-Ni-Fe alloys. *International Journal of Refractory Metals and hard materials*, 25(5-6), 380-385.

Joonwoong, N., Heungsub, S., Eunpyo, K., Woonhyung, B., Kilsung, C., & Kang, S. L. (1993). Matrix penetration of W/W grain boundaries and its effect on mechanical properties of 93W-5.6 Ni-1.4 Fe heavy alloy. *Metallurgical Transactions. A, Physical Metallurgy and Materials Science*, 24(11), 2411-2416.

Kiran, U. R., Venkat, S., Rishikesh, B., Iyer, V. K., Sankaranarayana, M., & Nandy, T. K. (2013). Effect of tungsten content on microstructure and mechanical properties of swaged tungsten heavy alloys. *Materials Science and Engineering: A*, 582, 389-396.

Kim, D. K., Lee, S., Ryu, H. J., Hyunghong, S., & Noh, J. W. (2000). Correlation of microstructure with dynamic deformation behavior and penetration performance of tungsten heavy alloys fabricated by mechanical alloying. *Metallurgical and Materials transactions A*, 31(10), 2475-2489.

Li, Y., Hu, K., Li, X., Ai, X., Qu, S. (2013). Fine-grained 93W-5.6Ni-1.4Fe with enhanced performance prepared by cyclic spark plasma sintering. *Mater. Sci. Eng. A*, 573, 245-252.

Li, X., Hu, K., Qu, S., Li, L., & Yang, C. (2014). 93W-5.6 Ni-1.4 Fe heavy alloys with enhanced performance prepared by cyclic spark plasma sintering. *Materials Science and Engineering: A*, 599, 233-241.

Liu, J., & German, R. M. (2001). Microstructure effect on dihedral angle in liquid-phase sintering. *Metallurgical and Materials Transactions A*, 32(1), 165-169.

Liu, W., Ma, Y., & Cai, Q. (2011). Consolidation of MA W-Ni-Fe alloyed powder by microwave-assisted sintering. *Materials Sciences and Applications*, 2(06), 609-614.

Liu, W., Ma, Y., & Zhang, J. (2012). Properties and microstructural evolution of W-Ni-Fe alloy via microwave sintering. *International Journal of Refractory Metals and Hard Materials*, 35, 138-142.

Ma, Y., Zhang, J., Liu, W., Yue, P., & Huang, B. (2014). Microstructure and dynamic mechanical properties of tungsten-based alloys in the form of extruded rods via microwave heating. *International Journal of Refractory Metals and Hard Materials*, 42, 71-76.

Prabhu, G., Kumar, N. A., Sankaranarayana, M., & Nandy, T. K. (2014). Tensile and impact properties of microwave sintered tungsten heavy alloys. *Materials Science and Engineering: A*, 607, 63-70.

Park, H. D., Baik, W. H., Kang, S. J. L., & Yoon, D. Y. (1996). The effect of Mo addition on the liquid-phase sintering of W heavy alloy. *Metallurgical and Materials Transactions A*, 27(10), 3120-3125.

Rabin, B. H., & German, R. M. (1988). Microstructure effects on tensile properties of tungsten-nickel-iron composites. *Metallurgical Transactions A*, 19(6), 1523-1532.

Upadhyaya, A., Tiwari, S. K., & Mishra, P. (2007). Microwave sintering of W-Ni-Fe alloy. *Scripta Materialia*, 56(1), 5-8.